SUPPLEMENTAL FIGURES

For

Tau aggregates are RNA-protein assemblies that mislocalize multiple nuclear speckle components.

Evan Lester, Felicia K. Ooi, Nadine Bakkar, Jacob Ayers, Amanda L. Woerman, Joshua Wheeler, Robert Bowser, George A. Carlson, Stanley B. Prusiner Roy Parker

Figure S1

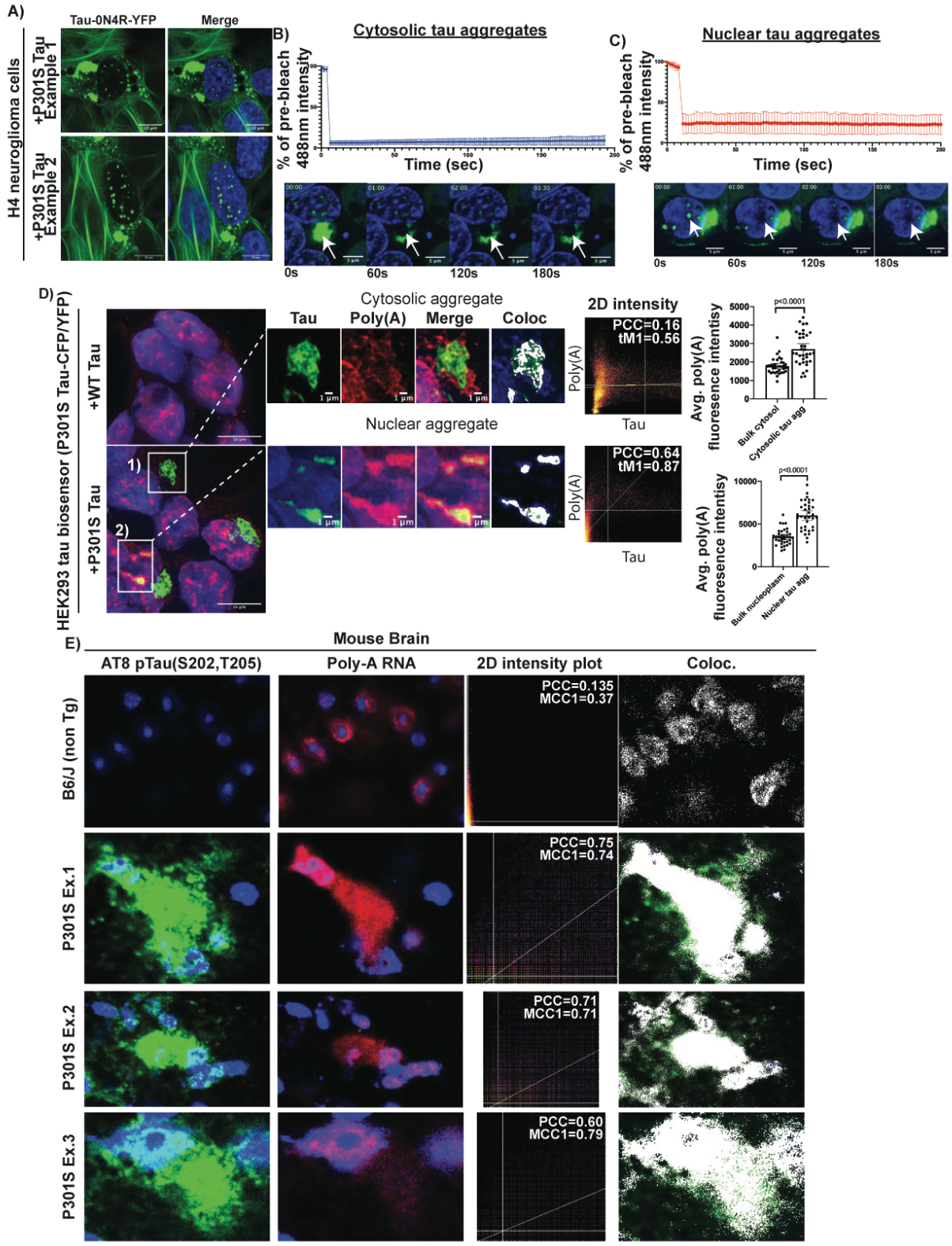
A)
Tau-0N4R-YFP
Merge
H4 neuroglioma cells
+P301S Tau Example 1
+P301S Tau Example 2
B)
Cytosolic tau aggregates
% of pre-bleach 488nm intensity
Time (sec)
0s
60s
120s
180s
C)
Nuclear tau aggregates
% of pre-bleach 488nm intensity
Time (sec)
0s
60s
120s
180s
D)
HEK293 tau biosensor (P301S Tau-CFP/YFP)
+WT Tau
+P301S Tau
1)
2)
Cytosolic aggregate
Tau
Poly(A)
Merge
Coloc
2D intensity
PCC=0.16
tM1=0.56
Poly(A)
Tau
Nuclear aggregate
PCC=0.64
tM1=0.87
Poly(A)
Tau
Avg. poly(A) fluoresence intentisy
p<0.0001
Bulk cytosol
Cytosolic tau agg
Avg. poly(A) fluoresence intentisy
p<0.0001
Bulk nucleoplasm
Nuclear tau agg
E)
Mouse Brain
AT8 pTau(S202,T205)
Poly-A RNA
2D intensity plot
Coloc.
B6/J (non Tg)
PCC=0.135
MCC1=0.37
P301S Ex.1
PCC=0.75
MCC1=0.74
P301S Ex.2
PCC=0.71
MCC1=0.71
P301S Ex.3
PCC=0.60
MCC1=0.79

Supplemental figure 1: FRAP of tau aggregates in HEK293 tau biosensor cells and additional examples of tau aggregates containing poly(A) RNA, related to figure 1. (A) H4 neuroglioma cells expressing 0N4R tau-YFP that contain nuclear tau aggregates. **(B, C)** FRAP of nuclear and cytosolic tau aggregates in HEK293 cells. 405 nm laser was used to photobleach and fluorescence intensity was measured in the 488cm channel (n=5). Arrow in example images shows bleached area. **(D)** FISH for poly(A) RNA in HEK293 cell nuclear and cytosolic tau aggregates**.** Bar graphs show quantification of poly(A) RNA fluorescence intensity within nuclear and cytosolic tau aggregates in relation to bulk cytosol and nucleoplasm. White pixels in Coloc image show pixels above the Costes determined thresholds in 2D intensity plots (PCC = Pearson correlation coefficient and tM1= thresholded manders colocalization (% of tau pixels above threshold that colocalize with poly(A) pixels above threshold)). Data are represented as mean ± 95% confidence intervals and significance was determined using an unpaired two-tailed t-test (N = 35 aggregates). **(E)** Additional examples from B6 non transgenic and P301S mice (Tg2541) showing cytosolic tau aggregates (Ex. 1) and nuclear tau aggregates (Ex. 2, 3) contain RNA.

Figure S2

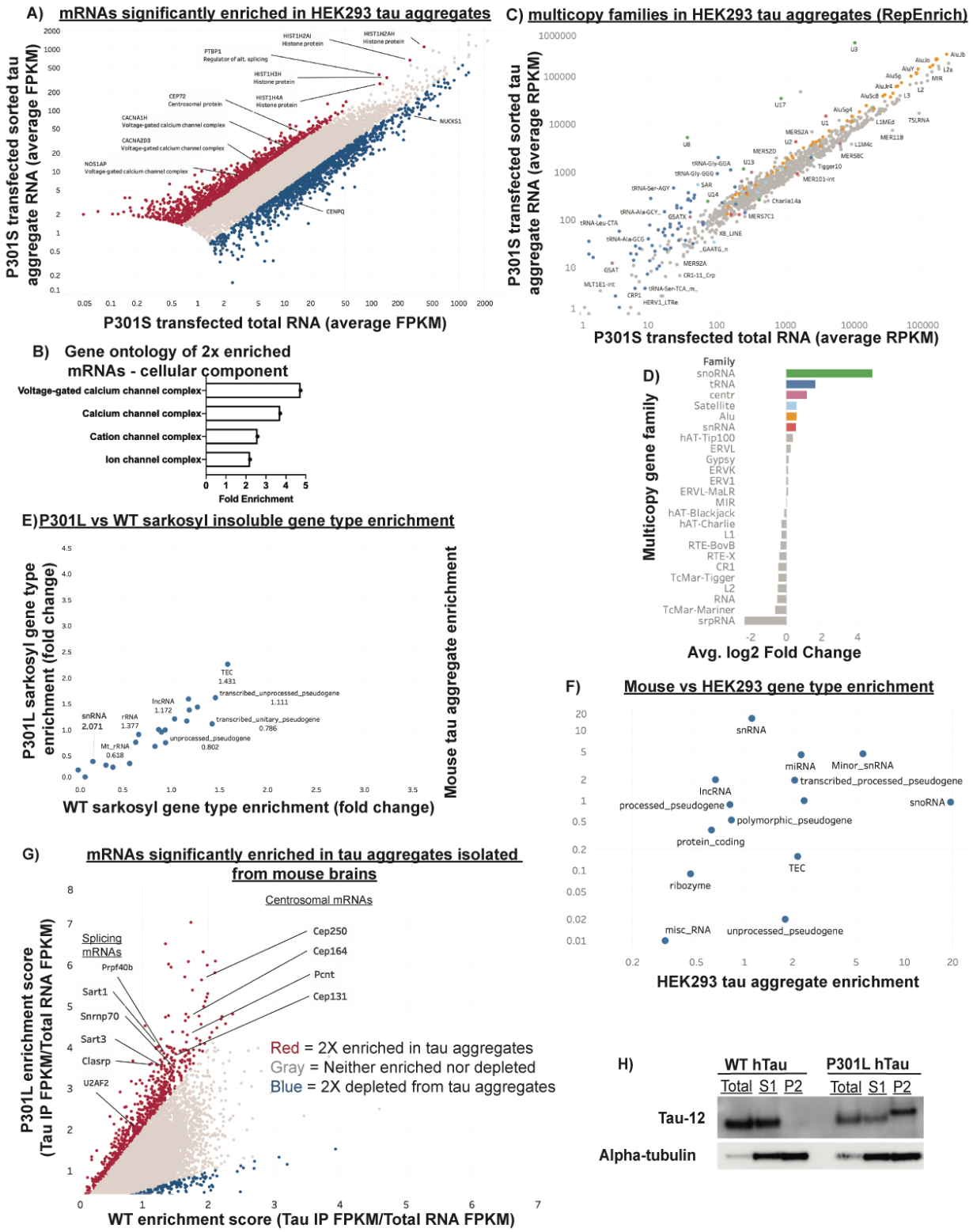
A) mRNAs significantly enriched in HEK293 tau aggregates
P301S transfected sorted tau aggregate RNA (average FPKM)
P301S transfected total RNA (average FPKM)
HIST1H2AI Histone protein
HIST1H2AH Histone protein
PTBP1 Regulator of alt. splicing
HIST1H3H Histone protein
CEP72 Centrosomal protein
HIST1H4A Histone protein
CACNA1H Voltage-gated calcium channel complex
CACNA2D3 Voltage-gated calcium channel complex
NOS1AP Voltage-gated calcium channel complex
NUCKS1
CENPQ
B) Gene ontology of 2x enriched mRNAs - cellular component
Voltage-gated calcium channel complex
Calcium channel complex
Cation channel complex
Ion channel complex
Fold Enrichment
C) multicopy families in HEK293 tau aggregates (RepEnrich)
P301S transfected sorted tau aggregate RNA (average RPKM)
P301S transfected total RNA (average RPKM)
D)
Family
Multicopy gene family
Avg. log2 Fold Change
E) P301L vs WT sarkosyl insoluble gene type enrichment
P301L sarkosyl gene type enrichment (fold change)
Mouse tau aggregate enrichment
WT sarkosyl gene type enrichment (fold change)
F) Mouse vs HEK293 gene type enrichment
HEK293 tau aggregate enrichment
G) mRNAs significantly enriched in tau aggregates isolated from mouse brains
Centrosomal mRNAs
Splicing mRNAs
Red = 2X enriched in tau aggregates
Gray = Neither enriched nor depleted
Blue = 2X depleted from tau aggregates
P301L enrichment score (Tau IP FPKM/Total RNA FPKM)
WT enrichment score (Tau IP FPKM/Total RNA FPKM)
H)
WT hTau
P301L hTau
Total S1 P2
Tau-12
Alpha-tubulin

Supplemental figure 2: Additional data on HEK293 and mouse brain tau aggregate isolation, related to figure 2. (A) Analysis of mRNAs two-fold enriched in tau aggregates from HEK293 cells (n = 2 replicates). Genes with fewer than 5 FPKM were removed from analysis due to low coverage. Genes from the following groups were highlighted: Voltage-gated calcium channel proteins, histone proteins, centrosomal proteins, and splicing related proteins. **(B)** Cellular component gene ontology of the mRNAs that are two-fold enriched in tau aggregates. **(C, D)** Analysis of multicopy gene families using RepEnrich showing enrichment of specific snoRNA repeats (U8, U17, and U3), snRNA repeats (U1 and U2), tRNA species, and Alu elements. The gene family color scheme is shared between C and D. **(E)** Gene type enrichment in the P301L and WT sarkosyl insoluble samples. Fold change for each gene type was calculated by dividing the percentage of total FPKM made up by each gene type in the sarkosyl insoluble fraction (P2) by the percentage of total FPKM made up by each gene type in the total RNA. The numbers below the gene type names indicate the P301L/WT enrichment. Note the absence of snRNA enrichment in the sarkosyl insoluble fraction (n=2 biologic replicates). **(F)** Mouse vs HEK293 gene type enrichment. **(G)** Scatter plot of mRNA enrichment in mouse brain tau aggregates in P301L and WT mice. Enrichment scores were calculated by dividing the insoluble tau IP FPKM by the total RNA FPKM for each replicate. mRNAs in red are two-fold enriched and mRNAs in blue are two-fold depleted from the P301L sarkosyl insoluble tau IP. Genes with fewer than 5 FPKM were removed from analysis due to low coverage. Two groups of mRNAs were highlighted: centrosomal proteins and splicing related mRNAs. **(H)** Western blot of fractions from tau aggregate isolation showing P2 fraction (sarkosyl insoluble fraction) enriches for insoluble tau that is present in the P301L mice and not the WT mice.

Figure S3

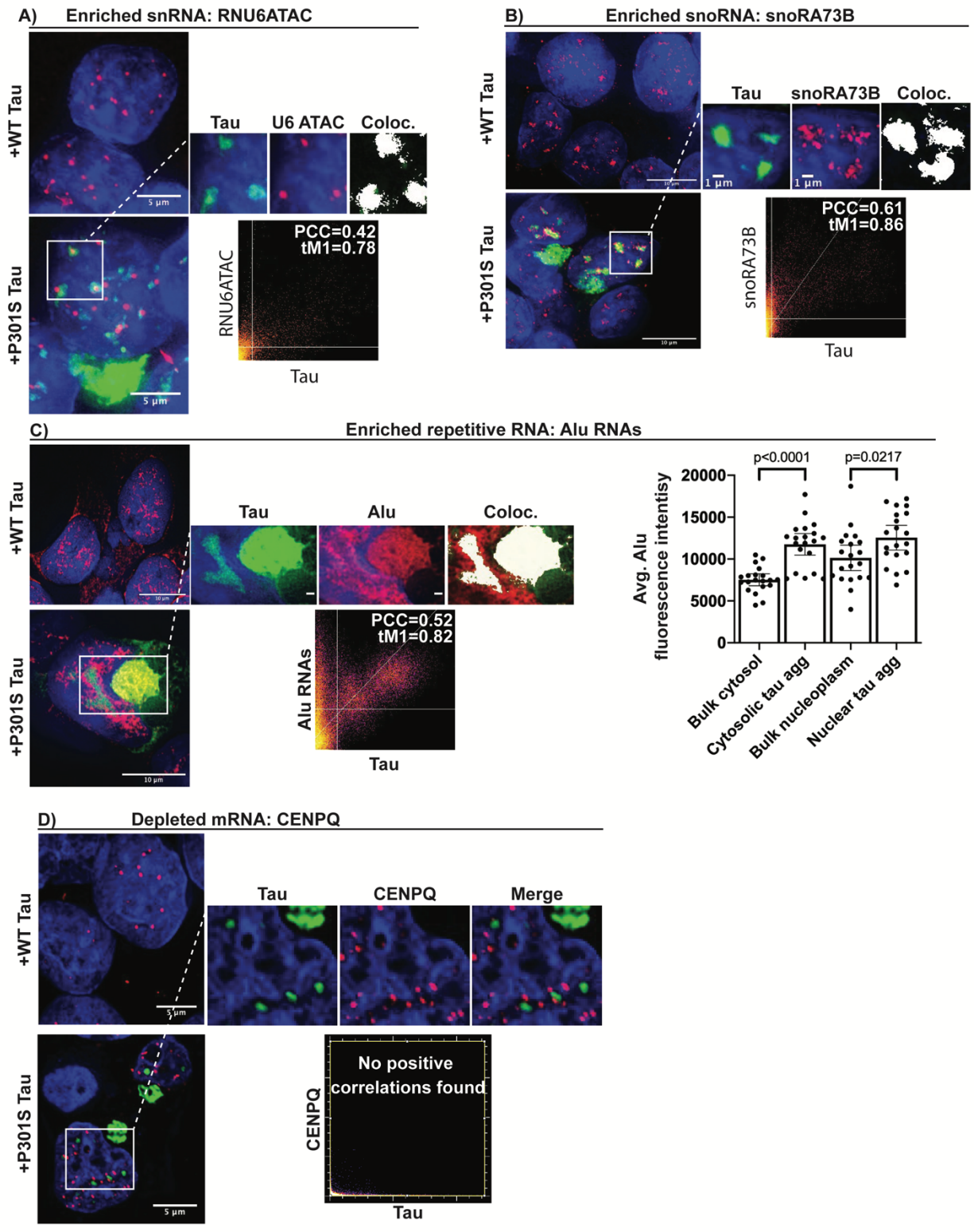
A)
Enriched snRNA: RNU6ATAC
+WT Tau
+P301S Tau
Tau
U6 ATAC
Coloc.
PCC=0.42
tM1=0.78
RNU6ATAC
Tau
B)
Enriched snoRNA: snoRA73B
+WT Tau
+P301S Tau
Tau
snoRA73B
Coloc.
PCC=0.61
tM1=0.86
snoRA73B
Tau
C)
Enriched repetitive RNA: Alu RNAs
+WT Tau
+P301S Tau
Tau
Alu
Coloc.
PCC=0.52
tM1=0.82
Alu RNAs
Tau
p<0.0001
p=0.0217
Avg. Alu fluorescence intentisy
20000
15000
10000
5000
0
Bulk cytosol
Cytosolic tau agg
Bulk nucleoplasm
Nuclear tau agg
D)
Depleted mRNA: CENPQ
+WT Tau
+P301S Tau
Tau
CENPQ
Merge
No positive correlations found
CENPQ
Tau

Supplemental figure 3: Additional FISH for RNAs in HEK293 tau biosensor cells, related to figure 3. (A, B) FISH of the enriched RNU6ATAC and snoRA73B shows overlapping fluorescence intensity in nuclear tau aggregates. **(C)** FISH for enriched multicopy Alu RNAs. Quantification shows enrichment in to nuclear and cytosolic tau aggregates, with greater enrichment into cytosolic tau aggregates relative to nuclear aggregates. Bar graphs show quantification of FISH fluorescence intensity within nuclear and cytosolic tau aggregates in relation to bulk cytosol and nucleoplasm. Data are represented as mean ± 95% confidence intervals and significance was determined using an unpaired two-tailed t-test (N=20 aggregates). White pixels in Coloc images show pixels above the Costes determined thresholds in 2D intensity plots (PCC = Pearson correlation coefficient and tM1= thresholded manders colocalization (% of tau pixels above threshold that colocalize with Alu FISH pixels above threshold)). **(D)** FISH for the depleted mRNA, CENPQ, reveals lack of enrichment in nuclear and cytosolic tau aggregates.

Figure S4

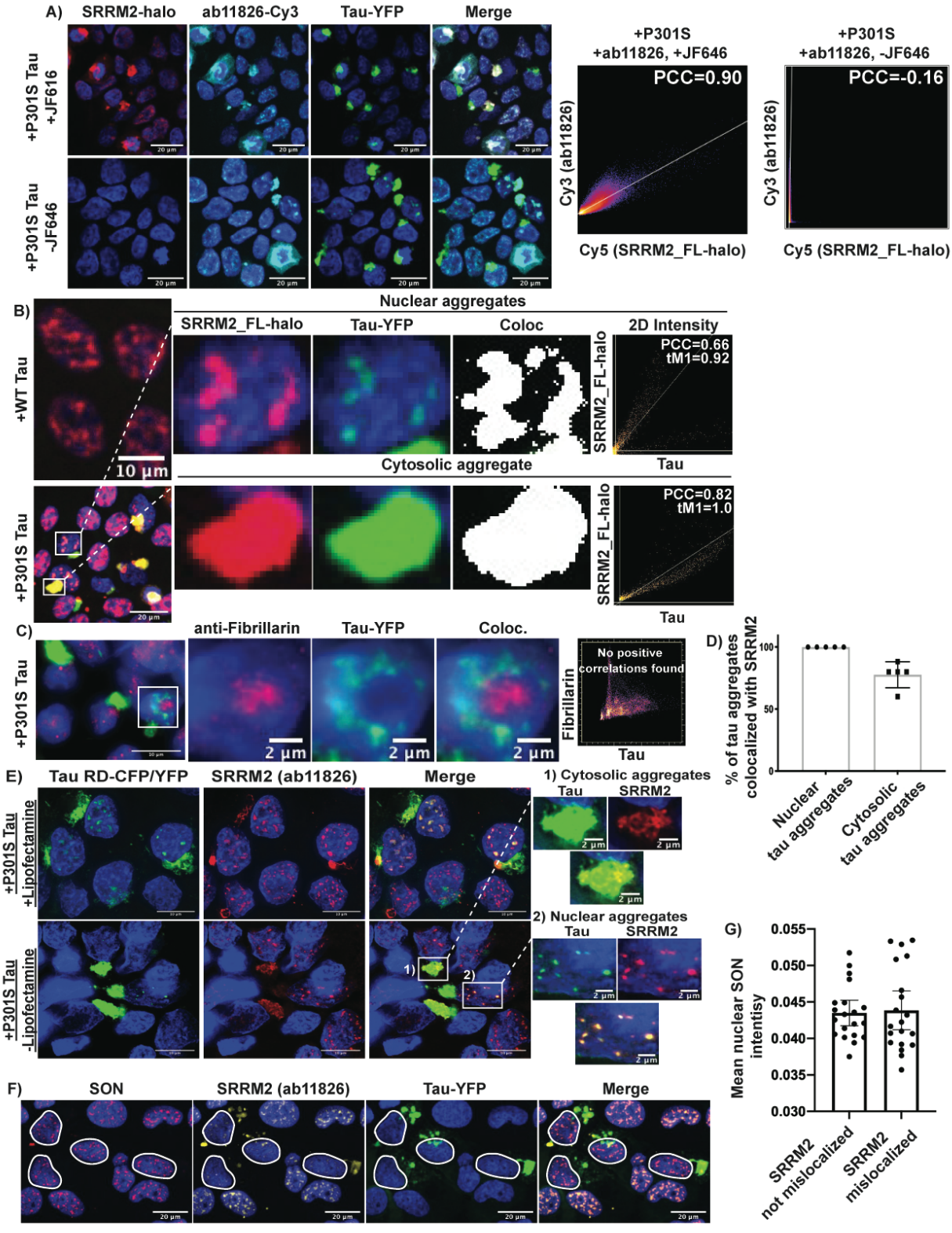
A)
SRRM2-halo
ab11826-Cy3
Tau-YFP
Merge
+P301S Tau +JF616
+P301S Tau -JF646
+P301S +ab11826, +JF646
PCC=0.90
+P301S +ab11826, -JF646
PCC=-0.16
Cy3 (ab11826)
Cy5 (SRRM2_FL-halo)
B)
Nuclear aggregates
SRRM2_FL-halo
Tau-YFP
Coloc
2D Intensity
PCC=0.66
tM1=0.92
+WT Tau
10 µm
Cytosolic aggregate
PCC=0.82
tM1=1.0
+P301S Tau
C)
anti-Fibrillarin
Tau-YFP
Coloc.
No positive correlations found
Fibrillarin
2 µm
D)
% of tau aggregates colocalized with SRRM2
Nuclear tau aggregates
Cytosolic tau aggregates
E)
Tau RD-CFP/YFP
SRRM2 (ab11826)
Merge
+P301S Tau +Lipofectamine
+P301S Tau -Lipofectamine
1) Cytosolic aggregates
2) Nuclear aggregates
F)
SON
SRRM2 (ab11826)
Tau-YFP
Merge
G)
Mean nuclear SON intentisy
SRRM2 not mislocalized
SRRM2 mislocalized

Supplemental figure 4: Additional HEK293 tau biosensor cell data, related to figure 4. **(A)** Colocalization analysis of SRRM2_FL-halo and ab11826 in HEK293 cells showing pearson correlation coefficient of 0.90. To control for channel bleed, the same analysis was performed without the JF646 halo ligand showing loss of colocalization and a decrease in the PCC to -0.16. **(B)** Images of HEK293 biosensor cells expressing SRRM2_FL-halo showing colocalization between nuclear and cytosolic tau aggregates. White pixels in Coloc. images show pixels above the Costes determined thresholds in 2D intensity plots (PCC = Pearson correlation coefficient and tM1= thresholded manders colocalization (% of tau pixels above threshold that colocalize with SRRM2_FL-halo pixels above threshold)). **(C)** IF for the nucleolar protein Fibrillarin showing lack of colocalization between tau aggregates and the nucleolus. Costes method was unable to identify a positive correlation to determine thresholds. **(D)** Analysis of the % of cytosolic tau aggregates that colocalize with SRRM2 in HEK293 tau biosensor cells. (n = 5 images, approximately 33 cells per image). **(E)** Tau aggregates form in both the nucleus and the cytosol with and without lipofectamine 2000 as a transfection reagent showing that SRRM2 mislocalization to cytosolic tau aggregates and nuclear tau aggregate formation are not dependent on lipofectamine. **(F, G)** Analysis of whether SRRM2 mislocalization disrupts the formation of SON positive splicing speckles. Cells outlined in white are cells that have SRRM2 mislocalized to the cytosol and by visual inspection and quantification of the average SON intensity, have no change in splicing speckles due to the mislocalization of SRRM2. Data are represented as mean ± 95% confidence intervals and significance was determined using an unpaired two-tailed t-test (n=20 measurements).

Figure S5

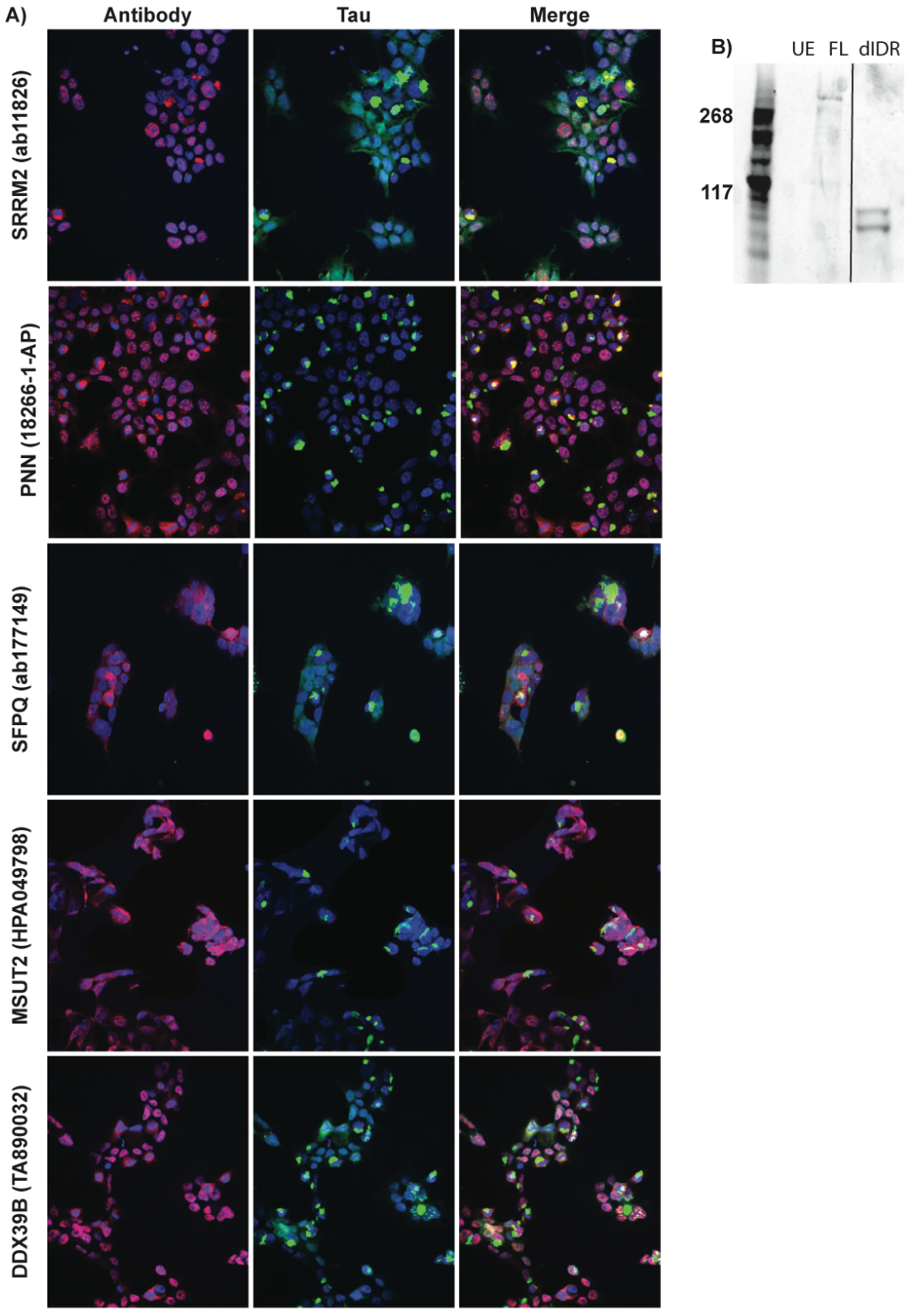
A)
Antibody
Tau
Merge
SRRM2 (ab11826)
PNN (18266-1-AP)
SFPQ (ab177149)
MSUT2 (HPA049798)
DDX39B (TA890032)
B)
UE
FL
dIDR
268
117

Supplemental Figure 5: Images of antibodies tested for enrichment in tau aggregates and truncation of SRRM2, related to figure 5. (A) Images of some of the proteins examined for their association with tau aggregates in Figs. 5 A, B. **(B)** Schematic of the halo tagged SRRM2 fusion proteins made using CRISPaint and gel showing JF647 conjugated to halo fusion constructs running at the appropriate sizes. All samples were run on the same gel, however the dIDR lane was not originally next to the FL lane and was placed next to it for clarity. The cut is indicated with a black line.

Figure S6

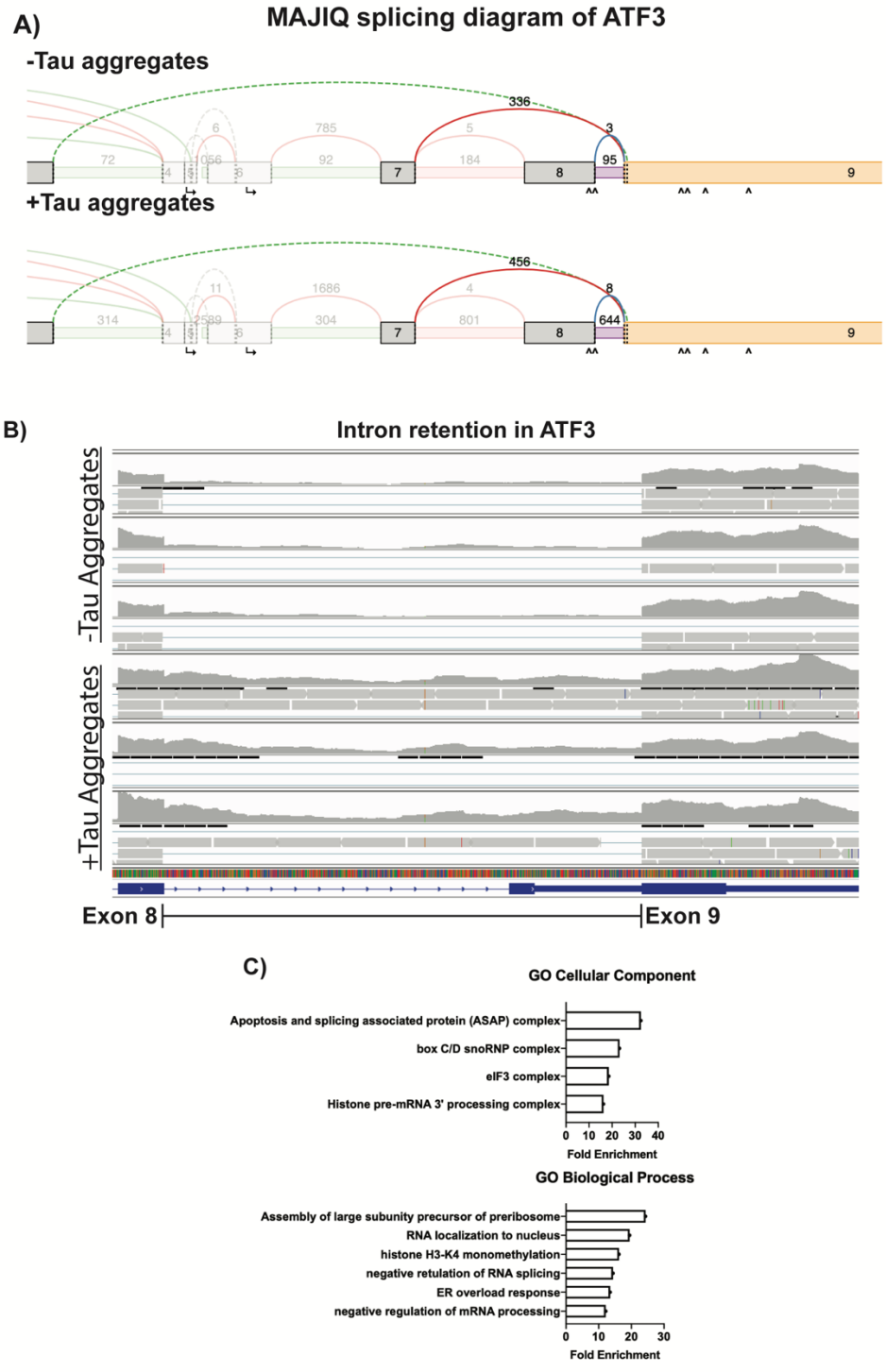
A)
MAJIQ splicing diagram of ATF3
-Tau aggregates
+Tau aggregates
B)
Intron retention in ATF3
-Tau Aggregates
+Tau Aggregates
Exon 8
Exon 9
C)
GO Cellular Component
Apoptosis and splicing associated protein (ASAP) complex
box C/D snoRNP complex
eIF3 complex
Histone pre-mRNA 3' processing complex
Fold Enrichment
GO Biological Process
Assembly of large subunity precursor of preribosome
RNA localization to nucleus
histone H3-K4 monomethylation
negative retulation of RNA splicing
ER overload response
negative regulation of mRNA processing
Fold Enrichment

Supplemental Figure 6: Additional splicing analysis data from cells with and without tau aggregates, related to figure 6. (A) Example of intron retention between exon 8 and 9 in ATF3 identified by MAJIQ at ΔPSI threshold of 0.1 and confidence threshold of 0.95. The numbers above the splice sites are normalized read counts and show the increase in reads mapping to the intronic region between exons 8 and 9 (644 vs 95) in cells with tau aggregates. **(B)** Integrated genome viewer image showing raw read counts for each sequencing replicate. Intron retention can be seen between exon 8 and 9. **(C)** Gene ontology of the genes containing significantly retained introns in cells with tau aggregates (FDR < 0.05).

Figure S7

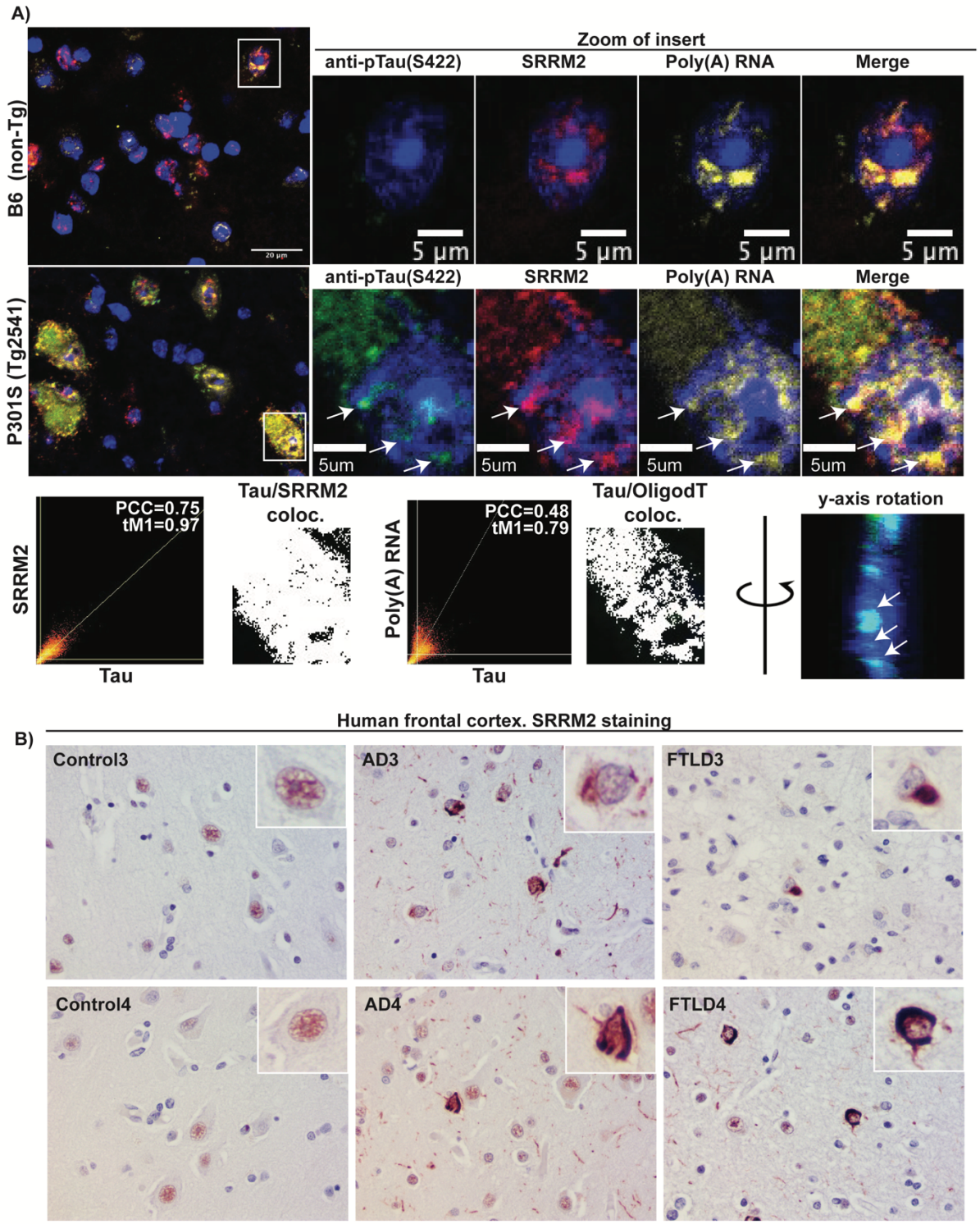
A)
Zoom of insert
anti-pTau(S422)
SRRM2
Poly(A) RNA
Merge
B6 (non-Tg)
P301S (Tg2541)
20 µm
5 µm
5um
PCC=0.75
tM1=0.97
SRRM2
Tau
Tau/SRRM2
coloc.
PCC=0.48
tM1=0.79
Poly(A) RNA
Tau
Tau/OligodT
coloc.
y-axis rotation
B)
Human frontal cortex. SRRM2 staining
Control3
AD3
FTLD3
Control4
AD4
FTLD4

Supplemental figure 7: Additional *in vivo* data from mouse and human tauopathies, related to figure 7. (A) IF and FISH showing p-tau (S422, ab79415) positive tau aggregates colocalized with SRRM2 (ab11826) and poly(A) RNA in the nucleus of Tg2541 mouse hindbrain. White pixels in Coloc images show pixels above the Costes determined thresholds in 2D intensity plots (PCC = Pearson correlation coefficient and tM1= thresholded manders colocalization (% of tau pixels above threshold that colocalize with red pixels above threshold)). Y-axis rotation shows that the pTau(S422) foci being interrogated in the zoomed images are within the nucleus rather than above or below the nucleus. **(B)** IHC in human brain showing cytosolic inclusions of SRRM2 (ab11826) in AD and FTLD patient brains, but not in control brains. (Patient demographics for this figure and Figure 6B can be viewed in Supplemental Table 3).